A&A 430, 9–17 (2005)
DOI: 10.1051/0004-6361:20041408

Astronomy & Astrophysics

On the magnetohydrodynamic stability of current-carrying jets

H. Baty

Observatoire Astronomique, 11 rue de l'Université, 67000 Strasbourg, France
e-mail: baty@astro.u-strasbg.fr

Received 4 June 2004 / Accepted 8 September 2004

Abstract. In the framework of ideal magnetohydrodynamics, we analyse the stability of jets carrying an electrical current. We focus on $m = \pm 1$ helical modes of hot flows (with approximate equipartition between thermal and magnetic energies) embedded in different helical magnetic field configurations. Two types of instability are simultaneously present, with magnetic current-driven modes dominating the Kelvin-Helmholtz (KH) modes when the magnetic pitch length parameter is smaller than approximately $0.1R_j$ (R_j being the jet radius). In the supermagnetosonic regime, the enhanced stability of KH modes due to the presence of the electrical current is much weaker than previously obtained for cold flows embedded in a linear force-free equilibrium configuration (Appl et al. 1992). On the other hand, KH modes of transmagnetosonic current-carrying jets appear to be more unstable than their uniformly magnetized current-free counterparts, leading to a mixed current-driven/KH instability branch in the limit of small fast Mach number for a magnetic field configuration dominated by the azimuthal component at the jet radius. Finally, we discuss the relevance of our results for interpreting numerical simulations aiming to explain the remarkable stability and flow coherence observed in many astrophysical jets.

Key words. instabilities – magnetohydrodynamics (MHD) – ISM: jets and outflows – galaxies: jets

1. Motivation

It is well established that the presence of a large-scale magnetic field is of crucial importance in accretion-disk-jet systems. Indeed, the interaction of the accretion flow with a magnetic field is an efficient mechanism to explain the launching of the jet (see Casse & Keppens 2004, and references therein). As jets launched in this way generally carry a poloidal electrical current, the associated toroidal magnetic field component provides the collimation of the ejected flow in a self-consistent way via the magnetic tension. In turn, the magnetic field configuration determines the stability of the jet against perturbations. The present work focuses precisely on this latter point, which is of crucial importance for understanding the remarkable stability of many observed astrophysical jets (see reviews by Birkinshaw 1991; and Ferrari 1998). This is the case of collimated flows emanating from young stellar objects (YSO) as well as from Active Galactic Nuclei (AGN) for Fanaroff-Riley type II sources (FRII), which show coherence over distances that are very long compared to their radial extents.

The stability of current-carrying jets has been examined by Appl & Camenzind (1992) in an ideal Magnetohydrodynamic (MHD) framework. They have considered supermagnetosonic flows embedded in three different magnetic equilibrium configurations: two carrying an electrical current, whereas the third was chosen to be current-free with a purely poloidal uniform field. The authors have shown that current-carrying jets are significantly more stable than their current-free counterparts, which are themselves partially stabilized compared to purely hydrodynamic jets for the same fast Mach number M_f taken on axis. It was found that short wavelength instabilities are efficiently suppressed by a magnetic field. Moreover, the additional enhanced stability due to the presence of the electrical current is particularly important for the Bessel Function Model (BFM): a factor of order 3 can be deduced from the maximum spatial growth rate value, compared to the current-free case (see Fig. 1 in Appl & Camenzind 1992) for $M_f = 3$. However, given our ignorance of the magnetic field structure, it is necessary to consider a wider variety of equilibrium configurations. For example, the BFM configuration represents a linear force-free equilibrium of minimum magnetic energy, thus it has favourable stability properties (Taylor 1986). Moreover, the modes studied by Appl & Camenzind (1992) are Kelvin-Helmholtz (KH) instabilities, driven by the relative kinetic energy between the jet and the ambient medium. Jets are also liable to magnetic instabilities driven by the electrical current (Appl 1996), with negligible growth rates for the BFM but not for more general force-free equilibrium configurations (Appl et al. 2000; Lery et al. 2000).

The aim of the present paper is to extend the results obtained by Appl & Camenzind (1992) and Appl (1996), by performing a linear stability analysis of transmagnetosonic/supermagnetosonic jets embedded in general current-carrying magnetic field configurations. We mainly consider two complementary classes of axisymmetric equilibrium configurations: a force-free one that has a constant twist of magnetic field lines as a function of the radius, and a constant B_z

(axial field component) case having a variable twist (note that in the cylindrical geometry approximation the toroidal and poloidal directions reduce to the azimuthal and axial ones respectively). A last MHD equilibrium configuration carrying a zero net total current inside the jet radius is also taken into consideration in this work for completeness. Contrary to the previously cited studies where mainly magnetically dominated (having zero thermal energy) flows were assumed, we address more realistic flows with energy equipartition (i.e. having thermal and magnetic energies that are of the same order of magnitude). The plasma-β giving the ratio of thermal to magnetic plasma pressure is thus taken to be of order unity, as obtained in jet launching simulations by Casse & Keppens (2004). In the present work we focus on the $m = \pm 1$ helical modes (m being the azimuthal wave mode number), as $m = \pm 1$ KH surface instabilities are believed to be the most dangerous for the integrity of astrophysical jets (Birkinshaw 1991; Ferrari 1998), and because the $m = \pm 1$ magnetic kink instability is the dominant current-driven (CD) mode (Appl et al. 2000; Lery et al. 2000). Note also that MHD instabilities driven by the thermal pressure gradient can also be present with non-negligible growth rates, but are beyond the scope of the present paper. The latter pressure modes are generally highly localized with high wavenumbers, playing probably a crucial role in feeding and sustaining the turbulence (Kersalé et al. 2000; Longaretti 2003). We also disregard the effect of internal jet rotation (Hanasz et al. 2000). Finally, we consider a velocity shear layer of small but non-vanishing thickness, contrary to the usual vortex-sheet approximation used in Appl & Camenzind (1992).

The paper is organized as follows. The different equilibrium configurations assumed in this paper as well as the numerical procedure are presented in Sect. 2. In Sect. 3 we show the results of the linear stability study for the supermagnetosonic and transmagnetosonic regimes. In particular, we examine the effect of the magnetic pitch value of the field lines on the results. Finally, we conclude and discuss the consequences of our findings in the context of the stability of astrophysical jets in Sect. 4.

2. Jet equilibrium configurations and numerical procedure

2.1. Flow and magnetic profiles

As observed jets are generally well collimated flows extending over very long distances (with respect to their radial extents) with very small opening angles, they can be approximated by an infinitely long cylindrical shape. The usual cylindrical coordinates (r, θ, z) are then used. Moreover, it is convenient to assume an axisymmetric flow profile,

$$V_z(r) = \frac{V_0}{2}\left[\tanh\left(\frac{R_\mathrm{j} - r}{a}\right) + 1\right], \tag{1}$$

where V_0 is the amplitude of the velocity shear, and a is the half-width of the shear layer situated at the jet radius R_j. Thus, the jet velocity is assumed to possess only a component in the axial direction and is separated from the static ambient medium (at $r > R_\mathrm{j}$) by a finite width layer. Nevertheless, we focus on the limit $a/R_\mathrm{j} \ll 1$ to facilitate the interpretation of our results (see the discussion in Sect. 4). In this work we neglect the rotation of the plasma jet. This latter assumption is generally used in most of the previous analyses, except in a paper suggesting that a local magnetorotational instability could be at work in some extragalactic jets (Hanasz et al. 2000). One can also refer to Bodo et al. (1989, 1996) for the effect of rotation on MHD stability.

This flow is embedded in a magnetic configuration that is assumed to be in MHD equilibrium,

$$\boldsymbol{J} \times \boldsymbol{B} = \nabla P, \tag{2}$$

where $\boldsymbol{J}$, $\boldsymbol{B}$, and P are the electrical current density, magnetic field, and thermal pressure respectively. Indeed, for a sufficiently slow spatial variation of the physical parameters of the ambient medium the jet is probably able to continuously adjust itself in a sequence of quasi-equilibria. Note that the vacuum permability is set to unity in our units. We therefore consider one-dimensional axisymmetric equilibrium configurations that can be defined in a convenient way using the pitch length parameter $P_\mathrm{i} = rB_z/B_\theta$, which is a measure of the twist of the magnetic field lines. More precisely, force-free equilibria representing a constant pitch class (I) are first retained. They are equivalently given by,

$$B_z = B_0 \frac{1}{1 + (r/P_\mathrm{i})^2}, \tag{3}$$

$$B_\theta = B_0 \frac{r/P_\mathrm{i}}{1 + (r/P_\mathrm{i})^2}, \tag{4}$$

$$P = P_0, \tag{5}$$

where B_0 and P_0 are the magnetic field and thermal pressure amplitudes taken on-axis respectively. A second class (II) that has a constant B_z component throughout the jet and the ambient medium is also considered,

$$B_z = B_0, \tag{6}$$

$$B_\theta = B_0 \frac{r/r_\mathrm{c}}{1 + (r/r_\mathrm{c})^2}, \tag{7}$$

$$P = P_0 - \frac{B_0^2}{2}\left(1 - \frac{1}{\left[1 + (r/r_\mathrm{c})^2\right]^2}\right), \tag{8}$$

where r_c is a characteristic length scale. Note that this latter equilibrium class is consequently non non-force-free as a pressure gradient is required to balance the magnetic tension due to the azimuthal component, and that the corresponding pitch parameter has an increasing radial parabolic variation,

$$P_\mathrm{i} = r_\mathrm{c}\left[1 + (r/r_\mathrm{c})^2\right]. \tag{9}$$

In these two classes (I and II), the total electrical current flowing in the jet itself ($r \leq R_\mathrm{j}$) is not forced to be zero. We thus assume that the current system has to be closed with a return current situated in the ambient medium. For completeness, we

additionally consider a force-free configuration (III), $P = P_0$, carrying a null total current inside the jet radius and given by

$$B_z = \sqrt{B_0^2 - \frac{1}{5} - x^2\,(1-x^2)^4 + \frac{1}{5}\,(1-x^2)^5}, \quad (10)$$

and

$$B_\theta = x\Big[1 - x^2\Big]^2, \quad (11)$$

if $r \leq R_\mathrm{j}$;

$$B_z = \sqrt{B_0^2 - \frac{1}{5}}, B_\theta = 0, \quad (12)$$

if $r > R_\mathrm{j}$, where $x = r/R_\mathrm{j}$. Note that this latter equilibrium has also been used to model the development of MHD instabilities in a solar coronal loop (Gerrard et al. 2002).

In this work, P_0, and the plasma density ρ_0, are set to unity. The plasma density is thus assumed to be constant throughout the jet and the ambient medium, giving a sonic speed on-axis $C_\mathrm{s} = \sqrt{\gamma P_0/\rho} = 1.29$ in our units. The jet radius is $R_\mathrm{j} = 1$. The magnetic field amplitude is chosen to be $B_0 = 1.29$ leading to a plasma-β value on axis equal to 1.2, close to unity. The values considered for V_0 can vary from case to case in correspondence with $M_\mathrm{f} = V_0/V_\mathrm{f}$ values, where $V_\mathrm{f} = \sqrt{V_\mathrm{A}^2 + C_\mathrm{s}^2}$, and V_A is the Alfvén velocity on the axis (equal to 1.29 in our units). The remaining parameters P_i, r_c, and a can vary from case to case. Varying P_i and r_c allows us to explore the effect of the pitch while varying a gives the effect of the shear layer width.

2.2. The numerical procedure

An ideal MHD stability analysis is performed using the ZYLSPEK code (Appl & Camenzind 1992; Appl 1996), in which an eigenvalue problem for an infinitely long cylindrical jet is solved using a normal mode expansion of the form $f(r)\exp[i(m\theta+kz-\omega t)]$ for the different perturbed quantities. m, k, and ω are the azimuthal wavenumber, axial wavenumber, and frequency respectively. Since one is interested only in instabilities due to the jet itself, we employ a free numerical boundary condition at $r = 2R_\mathrm{j}$ that represents radially outgoing decaying waves for large radii (see Appl & Camenzind 1992 for more details). A boundary condition $r\xi = 0$ on-axis (where ξ is the radial displacement) is also necessary to provide regularity. As a temporal approach is taken in the ZYLSPEK code, with a complex frequency $\omega = \omega_r + i\gamma$ and a real axial wavenumber k, the temporal linear growth rate γ of a mode specified by the wavenumbers (k, m) is then obtained in a natural way. However, a spatial approach (with a real frequency and a complex axial wavenumber) better takes account of the convective nature of the instabilities in such flowing plasmas. Nevertheless, a spatial growth rate K can be deduced through the use of the group velocity $v_\mathrm{g} = \mathrm{d}\omega_r/\mathrm{d}k$ by $K = \gamma/v_\mathrm{g}$ (see the discussion in Payne & Cohn 1985, on the validity of this formula).

3. Results

In this work, we restrict our attention to the $m = \pm 1$ modes. Indeed, $m = \pm 1$ KH instabilities that develop at the jet surface are believed to be the most dangerous ones for the integrity of the flow, because they involve large-scale distortions of the whole jet with a non-zero displacement of the axis. An example of this can be seen in the purely hydrodynamic simulations done by Bodo et al. (1995, 1998). Moreover, it has been shown that the magnetic instabilities driven by the presence of the electrical current are also dominated by the $m = \pm 1$ azimuthal mode numbers (Appl et al. 2000).

3.1. Supermagnetosonic flows

As the plasma flow in astrophysical jets is expected to smoothly pass through the slow, Alfvénic, and fast magnetosonic points, a rather wide range of fast Mach numbers must be explored. Let us first consider the super-magnetosonic regime, by taking for example $M_\mathrm{f} = 3$, or correspondingly $V_0 = 5.47$ in our units. In order to investigate the comparative stability of the different equilibria, we adopt the values $a = 0.05R_\mathrm{j}$ for the flow profile $V_z(r)$, $P_\mathrm{i} = 1/4R_\mathrm{j}$ in case of configuration (I), and $r_\mathrm{c} = 1/4R_\mathrm{j}$ in case of configuration (II). This leads to the same on-axis pitch value P_i equal to $1/4R_\mathrm{j}$ for the two equilibria. Figures 1 and 2 show the dispersion branches $K(k)$ for constant pitch (I) and variable pitch (II) respectively. For comparison, additional dispersion branches (solid line) obtained for a current-free configuration with a purely axial uniform magnetic field $B = B_z = 1.29$ are also displayed.

Before discussing these results in detail, one needs to identify the different curves. In a supermagnetosonic regime, the azimuthal mode number m being given, one usually distinguishes the KH instability branches by using the number of radial nulls N in the total pressure perturbation (see Birkinshaw 1991). The $N = 0$ curve corresponds to a called "ordinary", "fundamental", or "surface" mode (SM). This fundamental mode, which is the generalisation of the KH instability of a single shear layer, has a maximum perturbation amplitude that decreases away from the interface. On the contrary, $N > 0$ curves are representative of modes that affect the whole jet radius and that are usually called "reflection" or "body" modes (BM). These latter modes are typical of two-shear or cylindrical layer configurations, as they become unstable by resonant reflections at the jet boudary. They are also characterized by a minimum unstable axial wavenumber as they only exist for sufficiently small wavelengths that can fit into the jet diameter. This identification is illustrated in Fig. 3, where one can see the $m = -1$ radial displacement associated to the SM mode and first BM mode ($N = 1$) for configuration (I) (k values close to the one giving the maximum growth rate are considered) in correspondence with the curves displayed in Fig. 1. In Figs. 1 and 2 only the first BM branches are displayed for clarity, but unstable $N > 1$ BM modes (not shown) enter at successively higher wavenumbers as N increases. Moreover, an additional $m = -1$ instability branch is present for the two helical magnetic configurations (I and II). This latter branch is unambiguously identified as a current driven mode. The corresponding radial displacement displays a radically different radial variation as it is confined to the inner part of the jet radius (see Fig. 3). Moreover, we have also checked that such magnetic

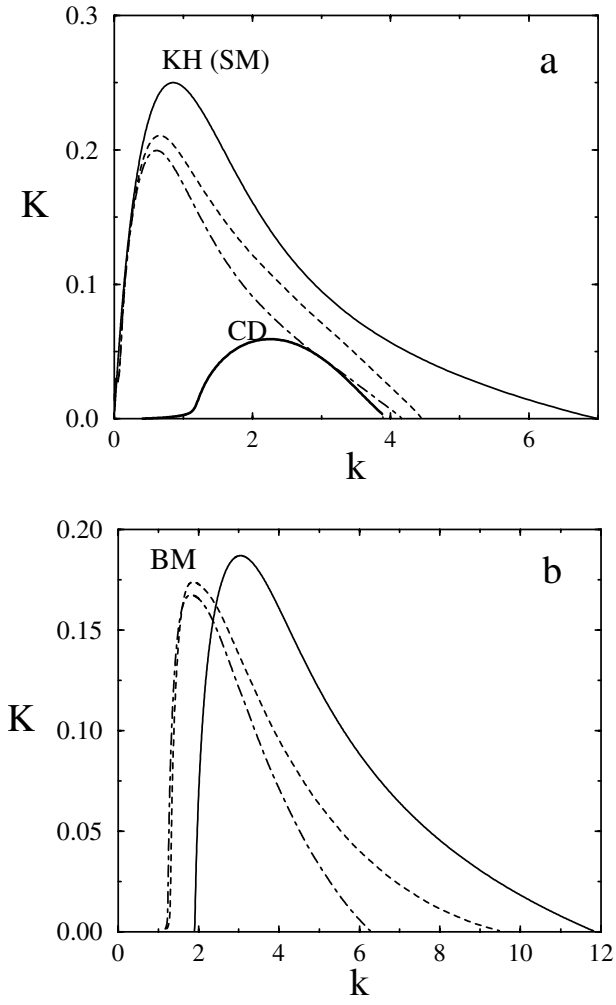

Fig. 1. Spatial growth rate K of the unstable $m = \pm 1$ modes as a function of the axial wavenumber k, for the constant twist configuration (I) with a pitch value $P_i = 1/4R_j$ and a fast Mach number $M_f = 3$. The different curves represent the $m = -1$ CD (thick solid line with label CD in a), $m = -1$ KH (dashed), and $m = +1$ KH modes (dash-dotted). For the KH instabilities, the SM and BM dispersion branches are displayed in a and b respectively. The KH (SM and BM) dispersion branches for a purely uniform-B_z configuration are also plotted for comparison (solid line in a and b respectively).

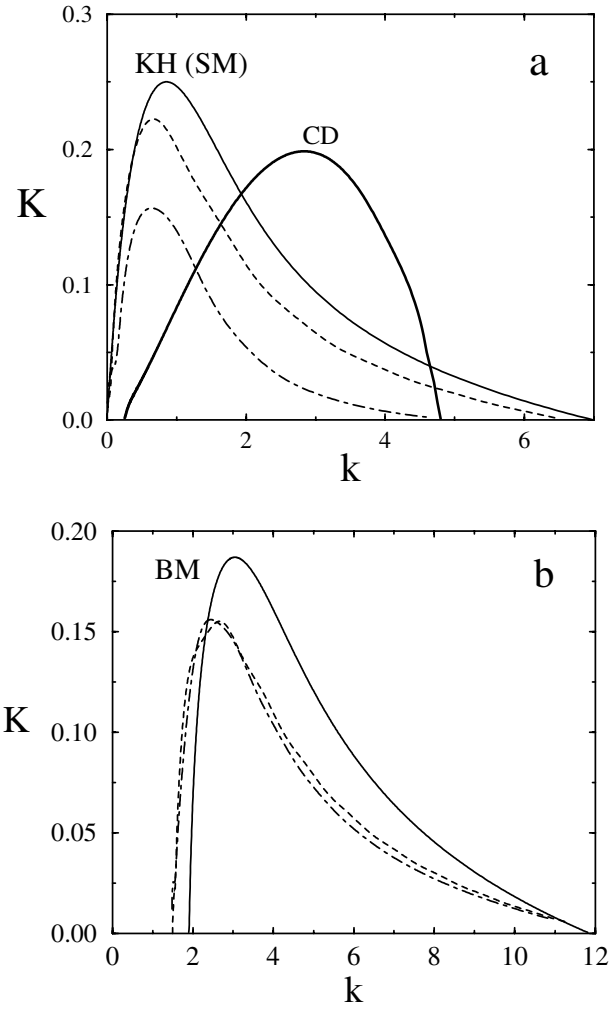

Fig. 2. Same as Fig. 1, for the helical magnetic configuration having a constant B_z component (II) with $r_c = 1/4R_j$.

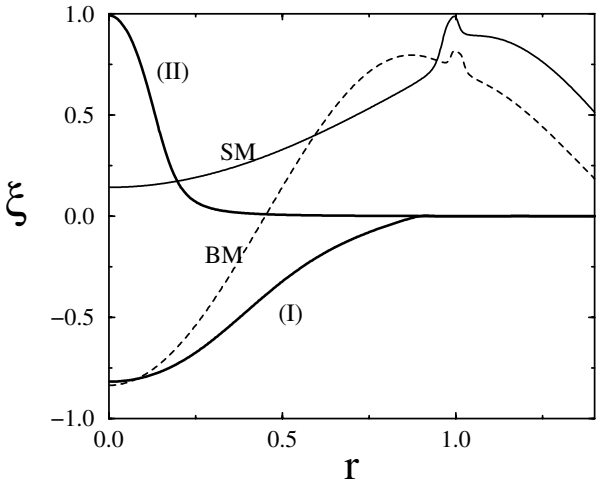

Fig. 3. Radial variation of the radial component of the $m = -1$ linear displacement $\xi(r)$. Shown are the CD modes (thick solid line) for the two configurations (I and II), surface KH (solid with label SM) and body KH (dashed with label BM) for the constant-pitch case (I). Arbitrary units are used for ξ. The jet radius is located at $r = R_j = 1$.

modes are convected at the jet velocity, contrary to the KH instabilities that propagate at only approximately half the jet velocity (Appl et al. 2000).

In Figs. 1a and 2a one must note that the degeneracy between the SM $m = +1$ and $m = -1$ modes is lifted in the presence of an helical magnetic field. Moreover, the $m = +1$ branch appears to be slightly stabilized compared to the $m = -1$ one, which is itself slightly stabilized compared to the $m = \pm 1$ SM current-free (uniform-B_z) branch. The same conclusion can be drawn for the BM modes (see Figs. 1b and 2b), even if the range of unstable k is additionally shifted towards smaller values. Another effect particularly visible for configuration (I) is that the modes become stable for large k values. An additional $m = -1$ branch that is identified to be a CD mode is also unstable (the CD $m = +1$ counterpart being stable), the highest growth rate being obtained for case (II). In order to investigate the effect of the finiteness of the total electric current flowing in the jet core, we have also reported in Fig. 4 the stability results

f4

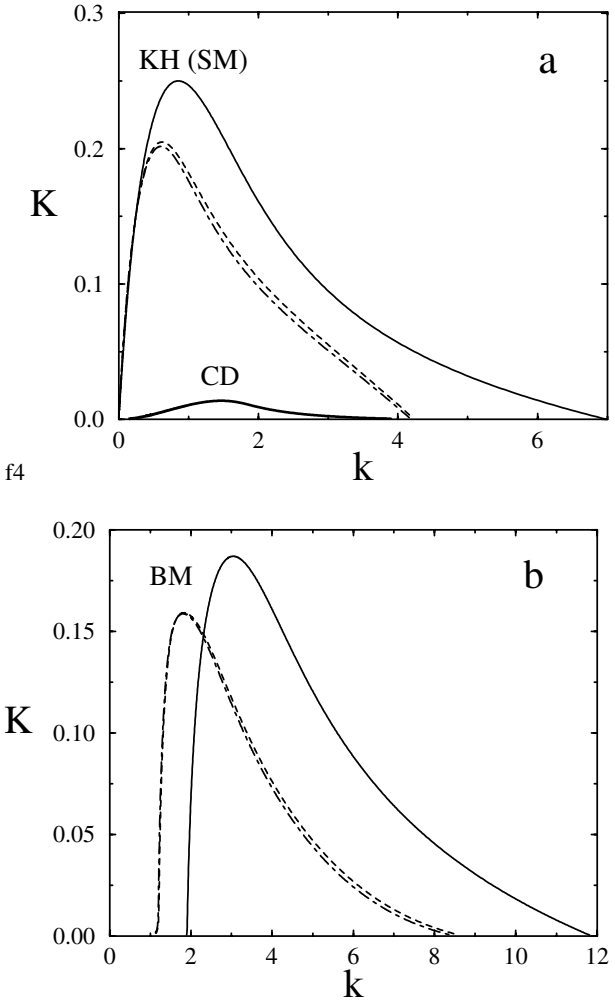

Fig. 4. Same as Fig. 1, for the helical magnetic configuration having a zero total net current (III).

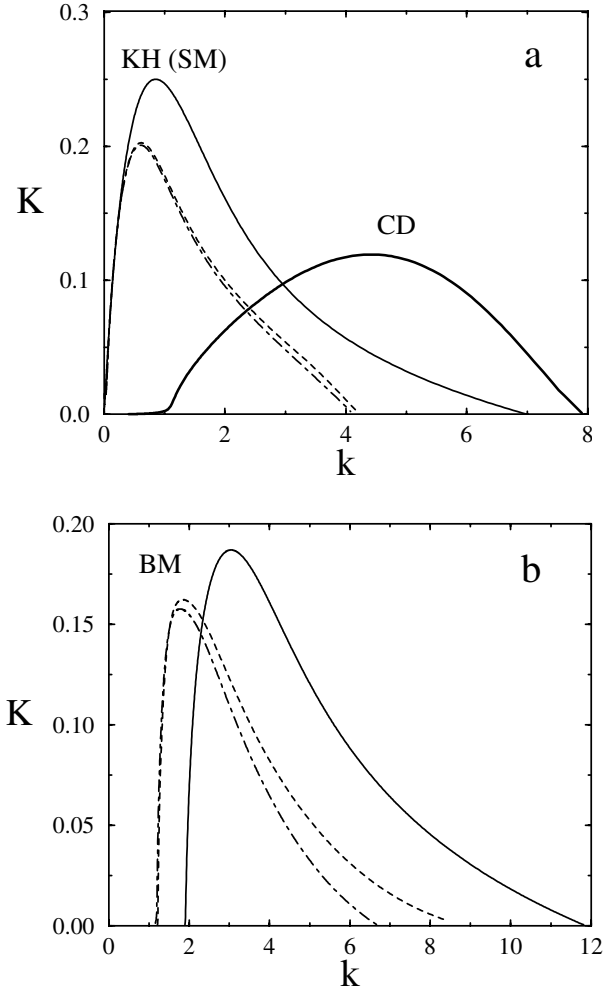

Fig. 5. Same as Fig. 1 with a pitch $P_\mathrm{i} = 1/8R_\mathrm{j}$.

obtained for configuration (III). Again, the results and consequently the previously drawn conclusions hold, except that the CD growth rate appears to be very low for this configuration because of the rather high pitch length value, equal to $1.29R_\mathrm{j}$ on-axis (see below).

Now we investigate the effect of the pitch value on the results. To do so, we can vary the parameters P_i and r_c in the two helical configurations (I and II) respectively. For example, in Fig. 5 one can see the effect of taking a pitch value that is twice as small, i.e. $P_\mathrm{i} = 1/8R_\mathrm{j}$ for the constant-pitch case. The KH branches are only slightly affected. This is not the case for the CD mode with a maximum growth rate K and a range of unstable k values that are increased by a factor of order 2 compared to the results reported in Fig. 1. The results for case (II) with $r_\mathrm{c} = 1/8R_\mathrm{j}$ are not shown because they lead to a similar conclusion. A more complete view of the pitch value dependence can be obtained from the results displayed in Fig. 6, where we plot the maximum growth rate K as a function of the inverse pitch $1/P_\mathrm{i}$ for the CD (cases I and II) and KH modes (case II only). Note that only the $m = -1$ KH (SM and BM) branches are considered, as the $m = +1$ counterparts follow the same behaviour. Only pitch values in the regime $P_\mathrm{i} \ll R_\mathrm{j}$ are investigated, as astrophysical jets are believed to possess magnetic configurations dominated by the azimuthal component over a large fraction of the jet radius (see discusion in Appl et al. 2000). This assumption is also reinforced by recent numerical simulations of jet launching from an accretion disk, where the pitch of the magnetic field lines that is obtained via the magneto-centrifugal process is lower than $0.2R_\mathrm{j}$ for more than 50 percent of the jet radius (Casse & Keppens 2004). From Fig. 6 one can easily observe that the CD growth rate scales linearly with the inverse of the pitch, while the SM rates are weakly sensitive to the pitch. This conclusion is in agreement with results previously obtained for the dominant CD instability in a cold ($P = 0$) constant twist configuration that was observed to grow with a linear dependence $K = 0.133V_a/(V_0P_\mathrm{i}) = 0.0314P_\mathrm{i}^{-1}$. The linear scalings deduced from Fig. 6 are different, i.e. $0.015P_\mathrm{i}^{-1}$ and $0.05P_\mathrm{i}^{-1}$ for cases (I) and (II) respectively. This is due to the destabilizing thermal pressure effect (the equilibrium pressure gradient being negative) that thus contributes to increasing the growth rate for case (II), while the perturbed thermal pressure (the equilibrium pressure being uniform) tends to reduce the growth rate for case (I), compared to a case in which the thermal pressure is absent.

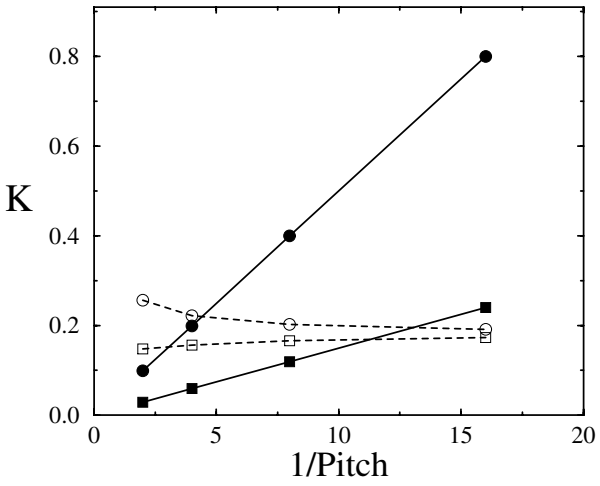

Fig. 6. Maximum spatial growth rate K of $m = -1$ instabilities as a function of the inverse pitch. Shown are the CD modes (filled squares and filled circles) for configurations (I and II) respectively, and Kelvin-Helmholtz modes (BM and SM with non-filled squares and circles respectively) for configuration (II).

In order to see the effect of considering a higher fast Mach number, we have computed the unstable branches for $M_{\rm f} = 6$ for a case similar to that obtained in Fig. 2 (with $M_{\rm f} = 3$). The results are displayed in Fig. 7. First, one must note the stability effect, enhanced by a factor of 2 on K for the different branches (compared to the $M_{\rm f} = 3$ case), is mainly a convection effect. Indeed, the spatial growth rate K is divided by two when a mode having a constant temporal growth rate is convected at a velocity that is twice as high. Second, the range of unstable axial wavenumbers k as well as the most unstable k are shifted towards lower values for the KH modes, contrary to the CD branch modes that are not affected. Nevertheless, the conclusions drawn previously for $M_{\rm f} = 3$ are unchanged.

We have also investigated the effect of varying the half-width a of the interface by taking a half-width shear layer $a = 0.1R_{\rm j}$ that is twice as large. The results (not shown) are not affected, except for the KH modes that have maximum growth rates reduced by a few percent. The range of unstable axial k wavenumbers is also slightly reduced, because the higher k are sensitive to the shear which thus render them stable only for $ka \gtrsim 1$ (Ferrari 1982), i.e. for $kR_{\rm j} \gtrsim 10$ for $a = 0.1R_{\rm j}$.

3.2. Transmagnetosonic flows

Let us now investigate the transmagnetosonic regime $0 \lesssim M_{\rm f} \lesssim 2$, following the rough definition used by Appl (1996). We first consider the case $M_{\rm f} = 1.5$ and perform a stability analysis for the same configurations (I and II with an on-axis pitch value equal to $0.25R_{\rm j}$) already studied in the supermagnetosonic regime. BM dispersion branches have dissappeared as BM modes become fully stabilized when $M_{\rm f}$ is lower than a critical value which is of order 2 for our configurations (see Bodo et al. 1989, 1996, for an analysis of the existence domain of body modes). We are thus left with KH surface and CD instabilities. The results showing the dispersion curves for configurations (I) and (II) are plotted in Figs. 8 and 9 respectively.

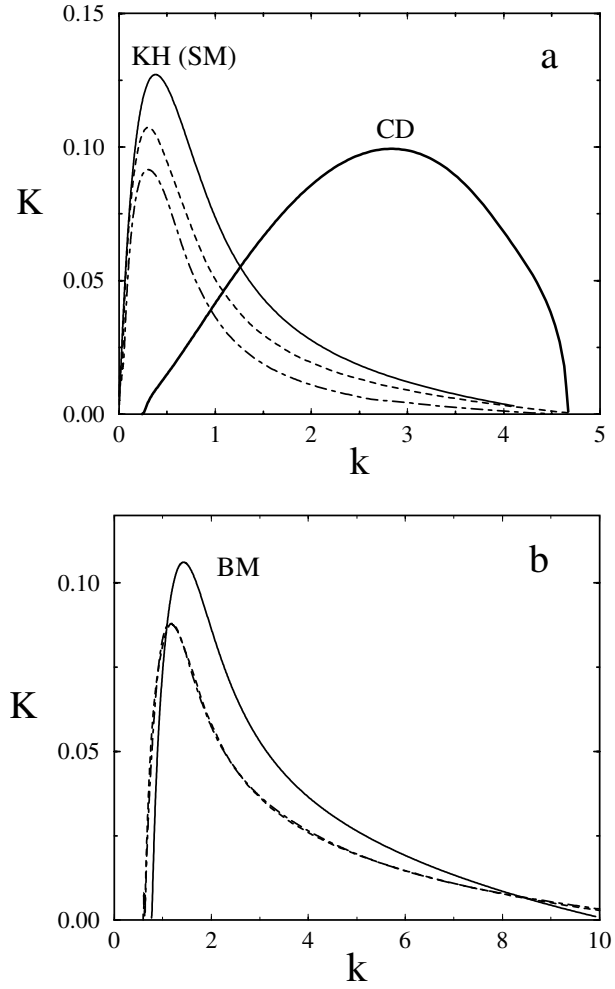

Fig. 7. Same as Fig. 2 with $M_{\rm f} = 6$.

First, one must note that the KH curve of the current-free constant-B_z configuration is now dominated by the SM dispersion branches of the helical configurations. Indeed, the corresponding Alfvén Mach number is $M_{\rm A} = V_0/V_{\rm A} = 2.12$ (on axis) for $M_{\rm f} = 1.5$, which is very close to the critical Alfvén Mach number value of 2 below which the KH surface instability in a uniform- B_z configuration is expected to become stable (Chandrasekhar 1961). This effect is particularly visible for the constant pitch case for which the $m = \pm 1$ KH modes largely dominate. However, while this result is also true for the $m = -1$ KH mode for configuration (II) (having a constant B_z) in a less spectacular way, the $m = +1$ KH counterpart is nearly stable. Moreover, for this latter (II) configuration, one must note that the dominant dispersion branch becomes the CD one, even though the pitch value is not so small. While the sensitivity of the CD mode to $M_{\rm f}$ is simply due again to the convection effect (compared to the $M_{\rm f} = 3$ case), this is less trivial for KH instabilities.

For completeness, we have also investigated the sensitivity of the unstable branches to $M_{\rm f}$ in the range $M_{\rm f} \ll 1$. First, the $m = -1$ CD branch becomes more and more unstable due to the convection effect as $M_{\rm f}$ decreases to zero. For the constant B_z case (II), the last KH instability to become fully stabilized as $M_{\rm f}$ is reduced is the $m = -1$ SM mode. This is clearly

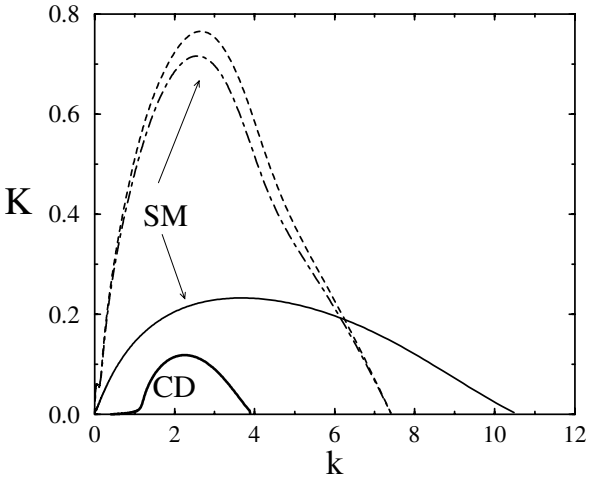

Fig. 8. Same as Fig. 1 with $M_{\rm f} = 1.5$. BM modes are stable.

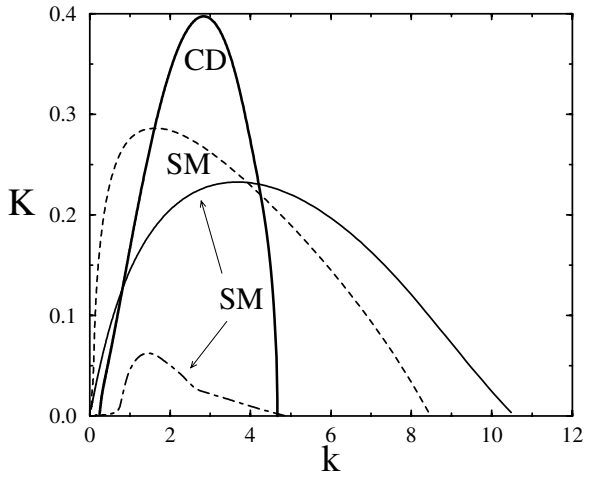

Fig. 9. Same as Fig. 2 with $M_{\rm f} = 1.5$. BM modes are stable.

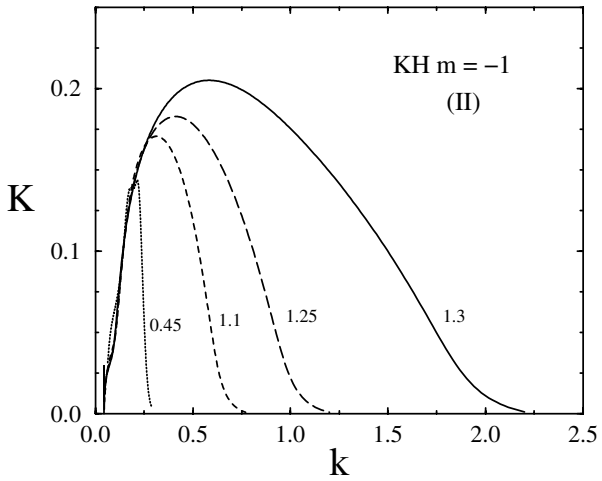

Fig. 10. Spatial growth rate K of the unstable $m = -1$ KH branch as a function of the axial wavenumber k, for the constant B_z configuration (II) with $r_{\rm c} = 1/4R_{\rm j}$. The different curves correspond to a transmagnetosonic regime with $M_{\rm f}$ ranging from 1.3 to 0.45 as indicated by the labels.

illustrated in Fig. 10, where the range of unstable k values situated on either side of a k value close to 0.23 is progressively reduced as $M_{\rm f}$ decreases. This can be understood by the examination of the expression $F = |\boldsymbol{V}\cdot\boldsymbol{k}|/|\boldsymbol{B}\cdot\boldsymbol{k}|$ evaluated at the jet interface ($\boldsymbol{k}$ being the wavevector of the mode). Indeed, this term enters in the stability analysis of a single "vortex sheet" (Chandrasekhar 1961). For example, in the simplest configuration for wich $\boldsymbol{B}$, $\boldsymbol{V}$, and $\boldsymbol{k}$ are parallel, a stability criterion is obtained when F is lower than a critical value close to 2. This means that a minimum magnetic field line tension is able to fully stabilize the KH mode. In the case of the current-free constant-B_z configuration, as F reduces to V_0/B_z, the stability criterion is $M_{\rm A} \lesssim 2$, or equivalently $M_{\rm f} \lesssim \sqrt{2}$ (as $C_{\rm s} = V_{\rm A}$). However, assuming the criterion remains valid for our cylindrical helical configurations, one has to examine the F expression for different k (m being given and equal to ±1 in our study). The behaviour of the current-carrying constant-B_z configuration (II) is the simplest to interpret in this respect. In this case, at the interface, the B_z component dominates over the azimuthal one B_θ component when $P_{\rm i} \ll R_{\rm j}$ (typically we have $B_z = 1.29$ and $B_\theta = 0.3$ for $P_{\rm i} = 1/4R_{\rm j}$). Our approximate stability criterion $F \lesssim 2$ is thus $V_0 \lesssim |2.58k \pm 0.6|/|k|$, $\pm$ corresponding to the $m = \pm1$ modes respectively. One can thus easily obtain that the $m = +1$ branch is fully stable when $V \lesssim 2.58$, which corresponds to $M_{\rm f} \lesssim 1.25$, in rough agreement with our results. As concerns the $m = -1$ mode counterpart, the last k value to become stable when $M_{\rm f}$ is reduced is $k = 0.232$ in agreement with Fig. 10, and this is obtained for $M_{\rm f} \ll 1$.

For the current-carrying constant pitch configuration (I), this stability criterion does not work, even if the tendency to have a complete stabilization for the KH branches is also observed when $M_{\rm f}$ is reduced to low values. This is due to the fact that the magnetic field is dominated by its azimuthal component at the jet radius, as $B_z = 0.076$ and $B_\theta = 0.3$. Moreover, an additional feature is obtained for the submagnetosonic regime $M_{\rm f} \ll 1$ when inspecting the unstable CD branch, as illustrated in Fig. 11. Indeed, whilst the maximum growth rate increases as $M_{\rm f}$ is reduced, k values situated in the range [0:1] suddenly become unstable for $M_{\rm f} \lesssim 0.3$. The lefthand part of this curve comes from the merging of the $m = -1$ KH with the CD one, due to a bifurcation that is beyond the scope of the present work. A mixed CD-KH branch is thus obtained, which is confirmed when one plots the associated radial displacement (not shown) that has a mixed nature.

4. Summary, outlook, and astrophysical relevance

We can summarize our findings as follows. First, we confirm that supermagnetosonic flows embedded in general helical magnetic configurations are partially stabilized compared to a purely axially uniform field with the same $M_{\rm f}$. The latter result concerns the $m = \pm1$ KH modes, that have maximum growth rates that are typically 10−20 percent lower than for the current-free uniform-B_z configuration. This stabilisation factor is much smaller than the value previously obtained (close to 70 percent) for cold jets embedded in a linear force-free BFM configuration (Appl & Camenzind 1992). In order to discuss the physical origin of this difference, we have additionally analyzed the stability of the force-free constant pitch

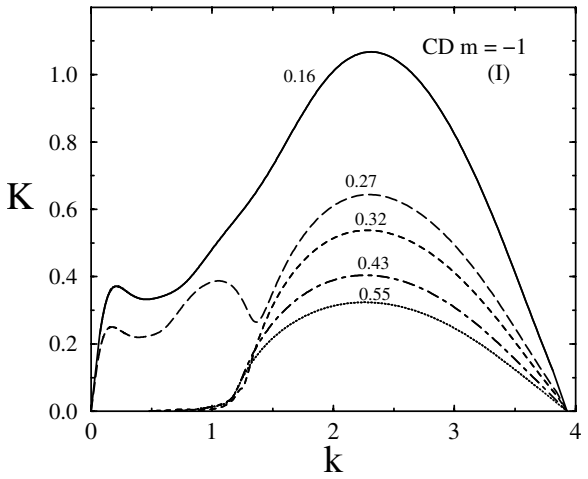

Fig. 11. Same as Fig. 10 for the $m = -1$ CD branch of the constant pitch configuration (I) with $P_\mathrm{i} = 1/4R_\mathrm{j}$. The different curves correspond to a submagnetosonic regime with M_f ranging from 0.55 to 0.16 as indicated by the labels.

configuration (I) for a low plasma-β ($\beta \ll 1$) at $M_\mathrm{f} = 3$. The results (not shown) give a stabilization factor of order 50 percent that is thus intermediate between the two previously cited ones. Therefore we can infer that the origin of the rather strong stabilization effect obtained by Appl & Camenzind (1992) is partly due to the assumption of a cold jet (in contrast to our results refering to hot jets with plasma-β of order unity). One can indeed understand that the stability properties are more sensitive to the magnetic configuration when the magnetic energy dominates the thermal one. The remaining difference from our results probably comes from the very particular properties of the BFM equilibrium. Indeed, this latter configuration is well known to be a state of minimum magnetic energy with a pitch parameter P_i that exhibits sign reversal at a radius situated inside the jet core, thus having favourable properties of stability (Taylor 1986). Moreover, we have shown the additional presence of well separated unstable branches, which are identified as $m = -1$ CD modes. These purely magnetic instabilities are very sensitive to the twist of the magnetic field lines. Indeed, their maximum growth rate scales linearly with the inverse of the pitch length parameter P_i, thus extending the previous results obtained for cold force-free jets (Appl et al. 2000). This is not the case for the KH modes that are only weakly dependent of the magnetic pitch. A comparative analysis of the relative importance of these two types of instability leads us to conclude on the dominance of CD over KH modes when the relative pitch $P_\mathrm{i}/R_\mathrm{j}$ is lower than a value of order 0.1 (see Fig. 6). We have checked that these results are not dependent on whether the return current is flowing in the external medium or in the jet core itself. In this work, we also confirm that the presence of an electrical current is destabilizing for KH modes developing in transmagnetosonic flows, as previously obtained for cold jets embedded in the BFM configuration (Appl 1996). While the body modes are already fully stable for $M_\mathrm{f} = 1.5$, SM branches of helical configurations remain unstable for M_f values smaller than unity. We recall that all KH instabilities are stabilized by the magnetic tension when $M_\mathrm{f} \lesssim \sqrt{2}$ for a (current-free) purely uniform-B_z configuration with a plasma-β of order unity. As concerns the magnetic modes, one is not surprised to see that unstable CD branches remain present for a vanishing jet velocity. However, for magnetic configurations having an azimuthal field component that dominates its axial counterpart, a mixed KH-CD unstable branch is obtained for M_f values typically smaller than a value of order 0.3 (not expected in the asymptotic collimated region of astrophysical jets). Finally, note that our results hold for flows having a small shear layer width $a/R_\mathrm{j} \ll 1$. This limit is usually assumed in most studies of collimated astrophysical flows. It is very useful in this work, as it mainly facilitates the interpretation of the results for the identification of the different instability branches. Indeed, the latter remain well separated, with for example the CD and SM Kelvin-Helmholtz modes confined to the jet core and interface respectively.

In the literature, the partial stabilisation during the linear phase of the development of the KH instabilities is evoked to explain various simulation results of supermagnetosonic jets embedded in helical magnetic fields. For example, this is the case for the numerical studies presented by Rosen et al. (1999) showing that in configurations having a moderately strong azimuthal magnetic field, jets are able to propagate without disruption over a distance much larger than their radial extent. This is not true for configurations with a dominant axial field (Hardee et al. 1997). However, on the basis of the results presented in the present paper, one must conclude that the linear enhanced KH stability is probably not sufficient to explain the differences between a helical field and a purely axial configuration. A non-linear stabilisation mechanism can also be at work, as shown for example by Baty & Keppens (2002) in high-resolution simulations of co-spatial shear flows and twisted magnetic fields. Indeed, it has been found that the nonlinear interaction between simultaneously growing KH and CD modes can in fact aid jet survival.

High-resolution simulations of purely hydrodynamic jets unambigously show how the KH instabilities nonlinearly lead to the disruption (with a turbulent transition) of the flow, on a time scale that is by far too rapid to reproduce the remarkable stability deduced from observations (Bodo et al. 1995, 1998). However, a MHD jet configuration allows a much richer complexity in the nonlinear evolution, which has only recently begun to be investigated in detail (Keppens & Tóth 1999; Ryu et al. 2000). For example, it has been shown that a self-organization process partially countered by small-scale reconnection events lead to the formation of large-scale coherent structures in an idealized single shear flow layer (Baty et al. 2003). The latter study has largely benefited from the use of an automated adaptive mesh refinement strategy to achieve a high resolution in numerical simulations. We must also mention other attempts to stabilize jets without resorting to magnetic fields, and invoking jet densities much higher than that of the surrounding medium and/or favourable radiative effects (Micono et al. 2000; Stone et al. 1997).

Recall that this work is mainly motivated by the discrepancy between observations of extended coherent astrophysical jets and the outcome of stability studies. The role played by the magnetic field topology in the survival of astrophysical jets to MHD instabilities remains an unsolved issue, and our stability

results indicate that this problem calls for nonlinear high resolution treatmentxs. Beyond this, the development of MHD instabilities could also be of crucial importance for explaining the morphological dichotomy in observed galactic jets (FRI jets appear turbulent and plumelike, while FRII jets remain well collimated). Finally, this is also the case for Herbig-Haro jets in YSO, for which the presence of helical magnetic fields is fundamental for explaining the production of knot-like structures due to the development of MHD instabilities (Thiele & Camenzind 2002).

Acknowledgements. The author is grateful to R. Keppens and F. Casse for helpful discussions, careful reading of the manuscript, and for providing him with details on the results obtained in Casse & Keppens (2004). We thank the anonymous referee for useful suggestions that help to clarify the content of the paper. This work was supported in part by the European Community's Human Potential Program under contract No. HPRN-CT-2000-00153, PLATON.

References

Appl, S., & Camenzind, M. 1992, A&A, 256, 354
Appl, S. 1996, A&A, 314, 995
Appl, S., Lery, T., & Baty, H. 2000, A&A, 355, 818
Baty, H., & Keppens, R. 2002, ApJ, 580, 800
Baty, H., Keppens, R., & Comte, P. 2003, Phys. Plasmas, 10, 4661
Birkinshaw, M. 1991, in Beams and jets in Astrophysics, ed. P. A. Hugues (Cambridge: Cambridge Univ. Press), 279
Bodo, G., Rosner, R., Ferrari, A., & Knobloch, E. 1989, ApJ, 341, 631
Bodo, G., Massaglia, S., Rossi, P., et al. 1995, A&A, 303, 281
Bodo, G., Rosner, R., Ferrari, A., & Knobloch, E. 1996, ApJ, 470, 797
Bodo, G., Rossi, P., Massaglia, S., Ferrari, A., Malagoli, A., & Rosner, R. 1998, A&A, 333, 1117
Casse, F., & Keppens, R. 2004, ApJ, 601, 90
Chandrasekhar, S. 1961, Hydrodynamic and Hydromagnetic Stability (New York: Oxford University Press)
Ferrari, A., Massaglia, S., & Trussoni, E. 1982, MNRAS, 198, 1065
Ferrari, A. 1998, Annual Rev. Astrophys., 36, 539
Gerrard, C. L., Arber, T. D., & Hood, A. W. 2002, A&A, 387, 687
Hanasz, M., Sol, H., & Sauty, C. 2000, MNRAS, 316, 494
Hardee, P. E., Clarke, D. A., & Rosen, A. 1997, ApJ, 485, 533
Kersalé, E., Longaretti, P.-Y., & Pelletier, G. 2000, A&A, 363, 1166
Keppens, R., Tóth, G., Westerman, R. H. J., & Goedbloed, J. P. 1999, J. Plasma Phys., 61, 1
Keppens, R., & Tóth, G. 1999, Phys. Plasmas, 6, 1461
Lery, T., Baty, H., & Appl, S. 2000, A&A, 355, 1201
Longaretti, P.-Y. 2003, Phys. Lett. A, 320, 215
Micono, M., Bodo, G., Massaglia, S., et al. 2000, A&A, 360, 795
Payne, D. G., & Cohn, H. 1985, ApJ, 291, 655
Rosen, A., Hardee, P. E., Clarke, D. A., & Johnson, A. 1999, ApJ, 510, 136
Ryu, D., Jones, T. W., & Frank, A. 2000, ApJ, 545, 475
Stone, J. M., Xu, J., & Hardee, P. E. 1997, ApJ, 483, 136
Taylor, J. B. 1986, Rev. Mod. Phys., 58, 741
Thiele, M., & Camenzind, M. 2002, A&A, 381, L53
Tóth, G. 1996, Astrophys. Lett. Commun., 34, 245